THE EVOLUTION OF OZONE OBSERVED BY UARS MLS IN THE 1992 LATE WINTER SOUTHERN POLAR VORTEX

Manney[1], Froidevaux[1], J. W. Waters, S. Elson[1],
Fishbein[1], R. W. Zurek[1], R. S. Harwood[2], V. A. Lahoz[2]

[1]Jet Propulsion Laboratory/California Institute of Technology,
Pasadena, CA

[2]Edinburgh University, UK

Abstract. The evolution of stratospheric ozone (O_3), as observed by the Microwave Limb Sounder on board the Upper Atmosphere Research Satellite, is described for 14 Aug through 20 Sep 1992, focusing on the polar regions. The formation of an ozone hole is observed, with minimum values of O_3 column above 100 hPa decreasing at high latitudes from ~17[illegible] DU on 14 Aug to ~110 DU on 20 Sep. A decrease of ~40% is seen in the average O_3 in the lower stratosphere from ~60 to 20 hPa within the polar vortex, and as much as 70% in the zonal mean near ~75° to 80°S. The average O_3 in the polar vortex in the mid-stratosphere, from ~10 to 3 hPa, increases by ~15%, with the zonal mean increasing by up to ~25% near 70°S and 7 - 5 hPa. Both horizontal and vertical transport appear to play a role in the mid stratospheric increase in O_3.

Introduction

The Microwave Limb Sounder (MLS) on board the Upper Atmosphere Research Satellite (UARS) measures concentrations of several species of interest in the middle atmosphere, including O_3 and ClO [Waters et al. 1993]. The satellite yaws at approximately one month intervals, providing coverage from ~30° latitude in one hemisphere to 80° latitude in the other. O_3 is measured on radiometers at 205 GHz and 183 GHz, with horizontal resolution of ~400 km and vertical resolution of ~4 km, throughout the stratosphere and lower mesosphere. The MLS instrument is described and retrieval methods summarized by Waters et al. [1993]. Validation of these data is still in progress. This letter describes results from initial analyses of data from the 205 GHz radiometer (V0003 file version); general conclusions are not expected to change with future processing updates.

These O_3 measurements provide unprecedented three-dimensional and temporal coverage of the polar winter stratosphere. Most previously available satellite data were limited to regions outside the polar night, and adversely affected by aerosols and ice clouds; aircraft data are limited in spatial coverage. During late winter 1992, the MLS took continuous measurements with coverage to ~80°S from 14 Aug through 20 Sep 1992. We show the time evolution of O_3 throughout the southern stratospheric polar vortex, in relation to meteorological quantities (potential temperature, winds, Rossby-Ertel potential vorticity) derived from National Meteorological Center (NMC) data.

Data and Analysis

The O_3 data are mapped to a latitude/longitude grid using Fourier transform techniques that separate time and longitude variations, as described by Salby [1982], and applied to MLS data by Elson et al. [1993]. Winds and Rossby-Ertel potential vorticity (PV) are calculated from NMC geopotential heights and temperatures as described by Manney and Zurek [this issue]. NMC temperatures are used to interpolate gridded MLS O_3 onto isentropic surfaces, since MLS temperatures are only available for pressures $\lesssim 22$ hPa; at these higher altitudes, little difference was noted in using MLS temperatures.

To estimate the amount of O_3 in the polar vortex near a given isentrope, we integrate the mass of O_3 in a volume bounded in the horizontal by a PV contour representative of the "edge" of the polar vortex, and in the vertical by a narrow layer ($\approx 2 - 2.5$ km) bounded by isentropes surrounding the desired level. This gives an estimate of the mass of O_3 in a thin slice of the vortex. The mass of air is estimated for the same volume;

dividing the mass of O_3 by the mass of air provides an average O_3 mixing ratio within the polar vortex. The PV contour used for integration is chosen by inspection at each level, and a "liberal" definition of the vortex is used, i.e., the contour is near the outside of the region of strong PV gradients that tends to isolate the polar vortex; the value used at each level is noted in Fig. . This calculation is generally insensitive to the exact PV contour and thickness of layer chosen.

Time Evolution of Ozone in the Polar Vortex

Figure 1 shows time series for 14 Aug through 20 Sep 1992 of the mass of O_3 (left, column 1), the mass of air (center, column 2) and average O_3 volume mixing ratio (right, column 3), for ten isentropic surfaces throughout the stratosphere. Column 2 gives a picture of the evolution of the polar vortex itself, similar to that shown in area integrals of PV [Butchart and Remsberg 986]; between 4 Aug and 20 Sep there is a decrease in polar vortex size at most levels. This decrease occurs gradually at the lower levels (465 K and 520 K). An abrupt decrease can be seen around Sep at higher levels, due to a minor stratospheric warming Fishbein et al., this issue], after which the vortex does not return to its former size at most levels. This sudden decrease appears earlier at higher levels, consistent with the warming starting in the upper stratosphere. The mass of O_3 in the vortex (column) also decreases in the lower stratosphere. While a general trend in O_3 mass is not obvious at higher levels, an abrupt decrease in mass is apparent at the time of the minor warming. The variations of columns and 2 will be similar to the extent that O_3 and PV are conserved tracers at these levels [Haynes and McIntyre 987

In column 3, we examine the average behavior of O_3 with respect to the vortex. In the lower stratosphere (465 K is near 50 to 60 hPa, and 520 K near 30 to 40 hPa at high latitudes), there is a steady decrease in O_3 mixing ratio. Waters et al. [this issue] show the behavior of ClO measured by MLS at 465 K; ClO values are high in the polar vortex throughout the time period studied. As described by Waters et al., the behavior of O_3 at these levels is consistent with the dominant effect being destruction by chlorine chemistry [e.g., Solomon, 1990]. However, it is apparent, especially at 465 K, that the decrease of 0_3 is slower at the beginning of this time period when ClO is highest [Waters et al., this issue], suggesting that dynamical effects may counteract some of the photochemical destruction of’ 0_3.

Between 740 K and 1300” K ($\approx$ 15 to 2 hPa), there is an increasing trend in 0_3 in the polar vortex, as is also apparent in renal means at 1 () and 5 hPa shown by Fishbein et al. this issue]. Trajectory calculations in a model simulation of this time period [Fisher et al., this issue] show horizontal particle motions in the upper stratosphere and mesosphere towards the center of the vortex, and strong diabatic descent in the. mid and upper stratosphere. At latitudes inside the polar vortex, vertical gradients of O_3 are relatively small above, and larger below $\approx$ 700 K. The direction of the gradients implies that O_3 is transported to all levels below approximately 1300 K by this descent. A number of studies of O_3 transport [e.g., Rood and Schoeberl 1983; Wu et al. 1987; Yang et al. 1991] show poleward and downward transport at these levels during winter and spring. In the upper stratosphere, O_3 is generally anti-correlated with temperature, since 0_3 in the upper stratosphere becomes more sensitive to local temperature-dependent photochemistry, which has short time scales compared to those for transport [e.g. Perliski et al., 1989]. Since the temperature is increasing in the upper stratosphere over the time studied, 0_3 is expected to decrease. This change to photochemically controlled behavior in the upper stratosphere is apparent for Aug-Sep 1992 in the flattening out of the O_3 trend in the uppermost level shown here.

At 585 K and 655 K, Figure 1 shows relatively little.cl~:tl~g,eitl 0_3 during this time period. Waters et al. [this issue] show that there are significantly elevated values of ClO at 22 and 46 hPa, near these levels, so other effects must compensate for chemical loss of 0_3. Since the vertical gradients of O_3 become larger near these levels, downward transport likely plays a significant role here,

Figure 2 shows a series of maps of O_3 and PV at 520 K and 960 K. Column O_3 above 100 hPa is also shown. Comparing values for 17 Aug and 17 Sep shows the large O_3 decrease in the polar vortex at 52(I K, and the O_3 increase at 960 K, as indicated in Fig. 1. The other maps shown are at 4 day intervals covering the time of the minor warming. On 5 Sep, near the peak of the warming, a large tongue of high O_3 is transported toward the pole near 1 40^{O}E longitude, and low O_3 is drawn off the edge of the vortex. Transport of low PV values into the polar region is also apparent. During this time, travelling and stationary wave 1 components intensify, leading to this distortion of the vortex, as described by Fishbein et al. [this issue]. Less pronounced transport into the polar regions is seen on other days. Column O_3 shows a steady decrease in the polar regions, mirroring that seen at 520 K. An increase in column O_3 outside the vortex region is also apparent, consistent with previous findings on the seasonal variation of O_3 [e.g., Yang et al. 1991]. The distortion of the polar vortex during the period of strong planetary wave activity is also apparent in column O_3.

Summary and Conclusions

Figure 3 summarizes the net changes in O_3 in the southern polar vortex in late winter 1992. Contours show the difference in zonal mean O_3 between 16 Aug and 19 Sep 1992. The bold lines show the region of strong I'V gradients, using a contour of zonal mean PV scaled in "vorticity units" so that the range of PV values is similar at all levels [Manney and Zurek, this issue], on 16 Aug (solid line) and 19 Sep (dashed line). O_3 decreases in the polar vortex between 420 K and 600 K due mainly to chemical destruction. An overall decrease in O_3 is seen as far equatorward as 40^{O} latitude, well outside the polar vortex, and as high as 740 K at high latitudes. There is a broad region in the mid to upper stratosphere where O_3 increases, with largest increase near 1100 K, where horizontal transport of O_3 during a minor stratospheric warming appears to play a role. The planetary wave activity associated with the warming is typical of the southern mid-stratosphere in late winter [Manney et al., 1991]. While quantitative estimates of transport are beyond the scope of this letter, the results shown here are consistent with previous studies suggesting that poleward and downward transport plays an important role in the mid-stratospheric increase in O_3.

Acknowledgments. Thanks to many MLS colleagues for their contributions to its success; to T. Luu for data management and graphics assistance, to P. Newman for supplying routines that were adapted to calculate PV. The UARS investigations were carried out by the Jet Propulsion Laboratory/California Institute of Technology under contract with NASA.

References

Butchart, N., and E. E. Remsberg, The area of the stratospheric polar vortex as a diagnostic for tracer transport on an isentropic surface, *J. Atmos. Sci., 43*, 1319-1339, 1986.

Elson, L. S., J. W. Waters, and L. Froidevaux, The use of Fourier transforms for asynoptic mapping: Early results from the Upper Atmosphere Research Satellite Microwave Limb Sounder, Submitted to *J. Geophys. Res.*, 1993.

Fishbein, E. F., L. S. Elson, L. Froidevaux, W. G. Read, J. W. Waters, G. L. Manney, and R. W. Zurek. MLS observations of stratospheric waves in temperature and ozone during the 1992 southern winter, Submitted to *Geophys. Res. Lett.*, 1993.

Fisher, M., R. Sutton, A, O'Neill, J. Russell III, A. Tuck, Rapid descent of mesospheric air into the stratospheric polar vortex, Submitted to *Geophys. Res. Lett.*, 1993.

Haynes, P. H., and M. E. McIntyre, On the evolution of vorticity and potential vorticity in the presence of diabatic heating and frictional or other forces, *J. Atmos. Sci.*, 44, 828-841, 1987.

Manney, G. L., J. D. Farrara, and C. R. Mechoso, The behavior of wave 2 in the Southern 1 Hemisphere stratosphere during late winter and early spring, *J. Atmos. Sci.*, 48, 976-998, 1991.

Manney, G. L., and R. W. Zurek, Interhemispheric Comparison of the development of the stratospheric polar vortex during fall: A 3-dimensional perspective for 1991-1992, Submitted to *Geophys. Res. Lett.*, 1993.

Perliski, L. M., S. Solomon, and J. London, On the interpretation of seasonal variations of stratospheric ozone, Planet, *Space Sci.* 37, 1527-1538, 1989.

Rood, R. B., and M. R. Schoeberl, Ozone transport by diabatic and planetary wave circulations on a beta plane, *J. Geophys. Res.*, 88, 8491-8504, 1983.

Salby, M. L., Sampling theory for asynoptic satellite observations, Part I: Space-time spectra, resolution and aliasing, *J. Atmos. Sci.*, 39, 2577-2600, 1982.

Solomon, S., Progress towards a quantitative understanding of Antarctic ozone depletion, Nature, 347, 347-354, 1990.

Waters, J. W., L. Froidevaux, W. G. Read, G. L. Manney, L. S. Elson, D. A. Flower, R. F. Jarnot, and R. S. Harwood, Stratospheric chlorine monoxide and ozone: First results from UARS MLS, Submitted to *Nature, 1993.*

Waters, J. W., L, Froidevaux, G. L. Manney, W. G. Read, and L. S. Elson, MLS observations of lower stratospheric ClO and O_3 in the 1992 southern hemisphere winter, Submitted to *Geophys. Res. Lett.*, 1993.

Wu, M.-F., M. A. Geller, J. G. Olson, and E. M. Larson, A study of global ozone transport and the role of planetary waves using satellite data, *J. Geophys. Res.*, 92, 3081-3097, 1987.

Yang, H., E. Olaguer, and K. K. Tung, Simulation of the present-day atmospheric ozone, odd nitrogen, chlorine and other species using a coupled 2-D model in isentropic coordinates, *J. Atmos. Sci.*, 48, 442-471, 1991.

Figure Captions

Figure **1.** Estimates of the mass of O_3 and air in selected layers of the polar vortex. The left column shows the mass of O_3 in a volume bounded in the horizontal by a PV contour defining the "edge" of the polar vortex, and in the vertical by two isentropic surfaces surrounding the labeled level that enclose a layer ≈ 2-2.5 km thick, The center column shows the mass of air in the same volume. The right column is the quotient of the left and center columns with appropriate scaling to give average O_3 volume mixing ratio in that layer of the polar vortex. The PV contour used to define the "edge" of the polar vortex at each level is given to the right of each row in units of 10^{-5} K $m^2 kg^{-1} s^{-1}$. See text for further details.

Figure 2. Synoptic maps of O_3 and PV at 520 K and 960 K, and the O_3 column above 100 mb, at 12 Z on selected days, The projection is orthographic, with the Greenwich meridian toward the top of the page; 30^{0} and 60° latitude circles are shown. O_3 is in ppmv, PV in 10-5 K $m^2 kg^{-1} s^{-1}$, and column O_3 in Dobson Units.

Figure 3. Change in zonal mean O_3 volume mixing ratio, and in the zonal mean representation of the polar vortex, between 16 Aug and 19 Sep 1992. Red shows the region of largest increase in O_3 and purple the region of largest decrease. The heavy solid line shows the position of the "zonal mean polar vortex" (see text) on 16 Aug, and the heavy dashed line its position on 19 Sep 1992.

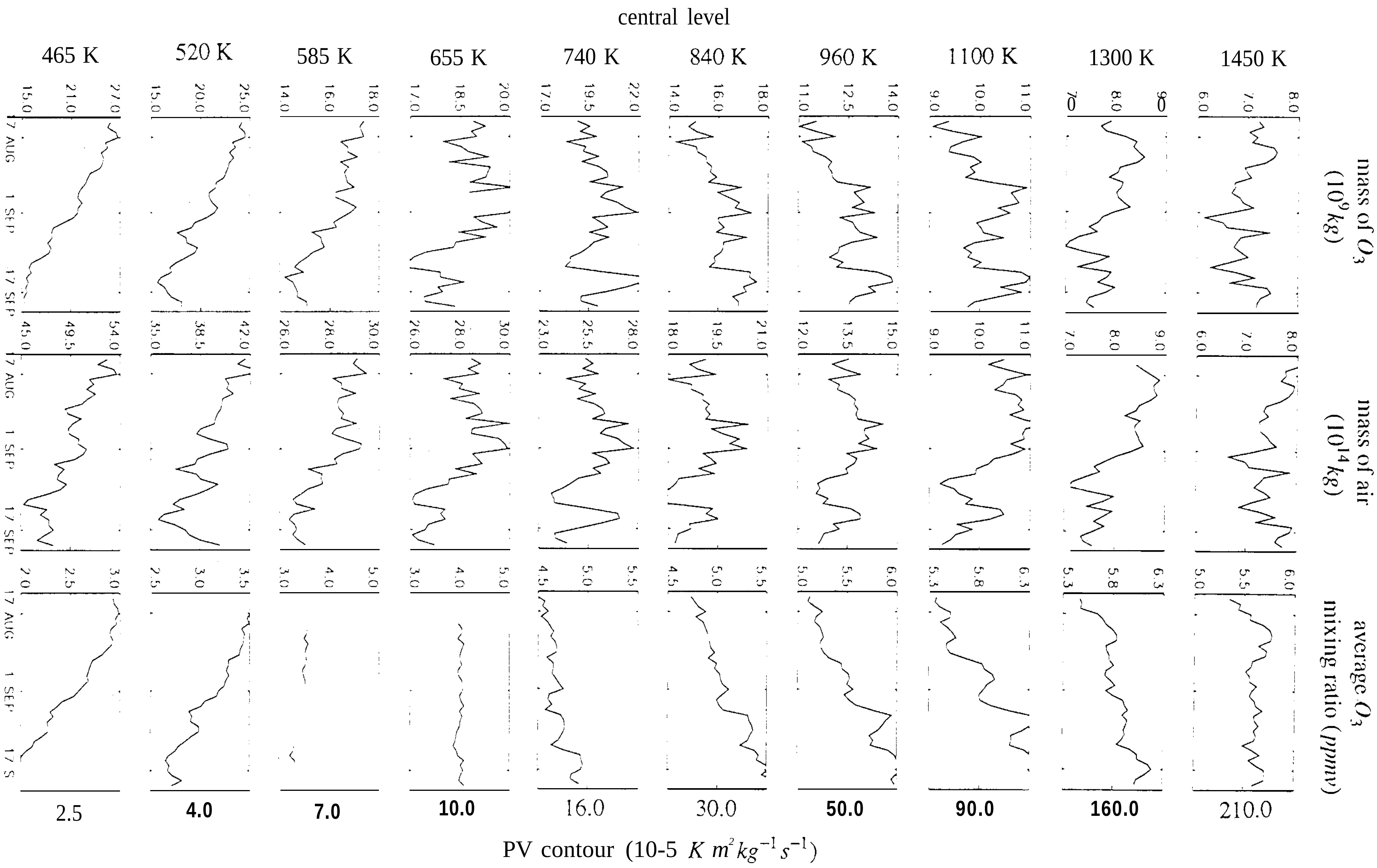
central level
465 K
520 K
585 K
655 K
740 K
840 K
960 K
1100 K
1300 K
1450 K
mass of O_3 ($10^9 kg$)
mass of air ($10^{14} kg$)
average O_3 mixing ratio ($ppmv$)
17 AUG
1 SEP
17 SEP
2.5
4.0
7.0
10.0
16.0
30.0
50.0
90.0
160.0
210.0
PV contour (10-5 $K\ m^2 kg^{-1} s^{-1}$)

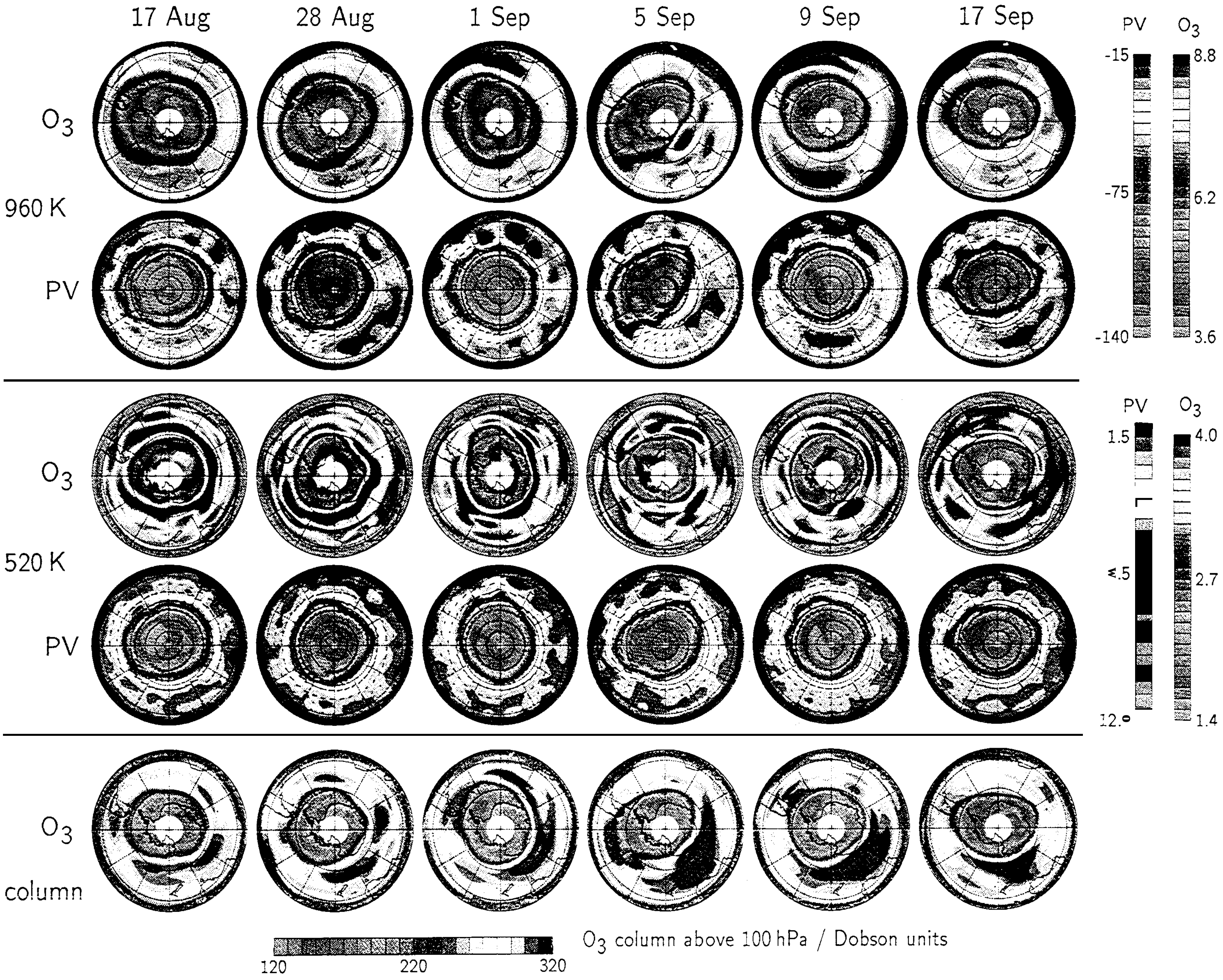
17 Aug
28 Aug
1 Sep
5 Sep
9 Sep
17 Sep
O$_3$
960 K
PV
O$_3$
520 K
PV
O$_3$
column
PV
O$_3$
-15
-75
-140
8.8
6.2
3.6
PV
O$_3$
1.5
4.5
12.0
4.0
2.7
1.4
120
220
320
O$_3$ column above 100 hPa / Dobson units

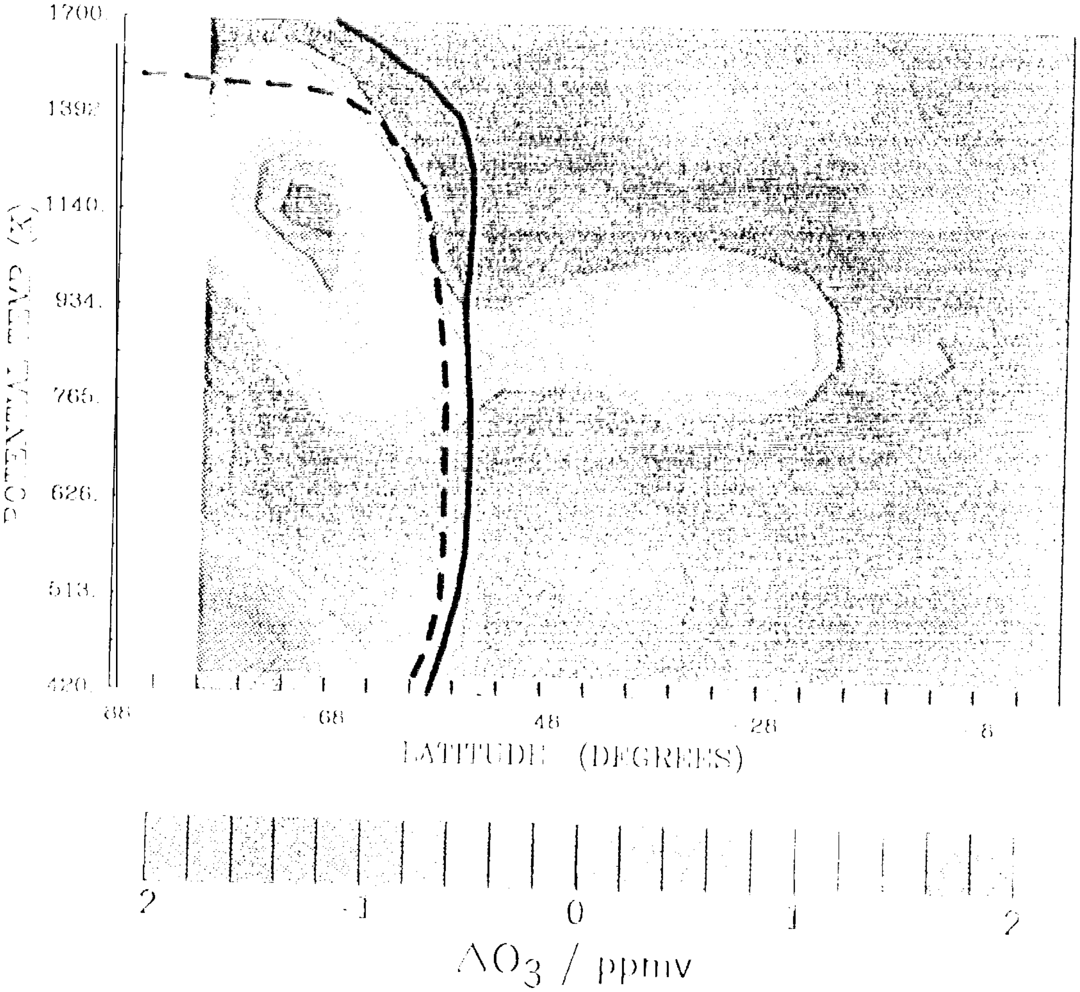
1700.
1392
1140.
934.
765.
626.
513.
420.
POTENTIAL TEMP (K)
88
68
48
28
8
LATITUDE (DEGREES)
2
-1
0
1
2
ΔO_3 / ppmv